

DIVISION OF BRAIN BIOLOGY



Professor
YAMAMORI, Tetsuo



Associate Professor
WATAKABE, Akiya

Assistant Professor: KOMINE, Yuriko
SADAKANE, Osamu

Assistant Professor (Specially appointed):
KOMATSU, Yusuke#
OHTSUKA, Masanari

NIBB Research Fellow: OHTSUKA, Masanari

Technical Staff: OHSAWA, Sonoko

Postdoctoral Fellow: TAKAJI, Masafumi#
OHTSUKA, Masanari*
HATA, Katsusuke#
SASAKI, Tetsuya
HIRAKAWA, Reiko

Visiting Scientist: SHUKLA, Rammohan

Graduate Student: NAKAMURA, Tohru

Technical Assistant: TAKEDA, Yuta#
NAKAGAMI, Yuki
MORITA, Junko
IMAI, Akiko
KOTANI, Keiko
KON, Yayoi
IMOTO, Eiko
HIRAYAMA, Yuka#
KAJITANI, Tomoki#
TAKAHASHI, Yoichi#

#: SRPBS (Strategic Research Program for Brain Sciences), NIPS

We continue to study genes that are expressed in specific areas of the neocortex in order to understand the principles governing the formation of the primate brain. In addition, this year we have reported a novel genetic manipulation method to visualize cortical projection neurons with retrograde TET-off lentiviral vector, area-specific substratification of deep layer neurons in the rat cortex, and the behavioral analysis of *zfhx2*-deficient mice as follows.

I. Area-specific substratification of deep layer neurons in the rat cortex

To identify cell types for fine mapping of neuronal circuits, we studied area-specific sublamina structures of the rat cerebral cortex using cholecystokinin (*cck*) and purkinje cell protein4 (*pcp4*) mRNAs as the markers for the subtypes of excitatory neurons in layers 5 and 6. We found a segregated expression, especially pronounced in layer 6, where corticothalamic and corticocortical projecting neurons reside (Figure 2). To examine the relationship between gene expression and projection target, we injected retrograde tracers into several thalamic subnuclei, ventral posterior (VP), posterior (PO), mediodorsal (MD), medial and lateral geniculate nuclei (MGN and LGN); as well as into two cortical areas (M1 and V1). This combination of tracer-in situ hybridization (ISH) experiments revealed that corticocortical neurons predominantly express *cck* and corticothalamic neurons predominantly express *pcp4* mRNAs in all areas tested. In general, *cck*(+) and *pcp4*(+) cells occupied the upper and lower compartment of layer 6a, respectively. However, the sublaminal distribution and the

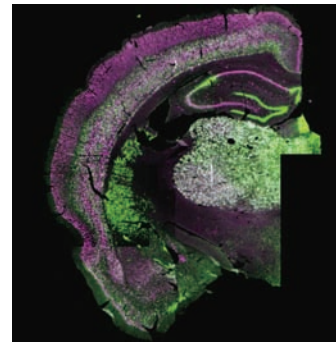


Figure 1. Cover letter for J. Comp. Neurology, Volume 520, Issue 16.

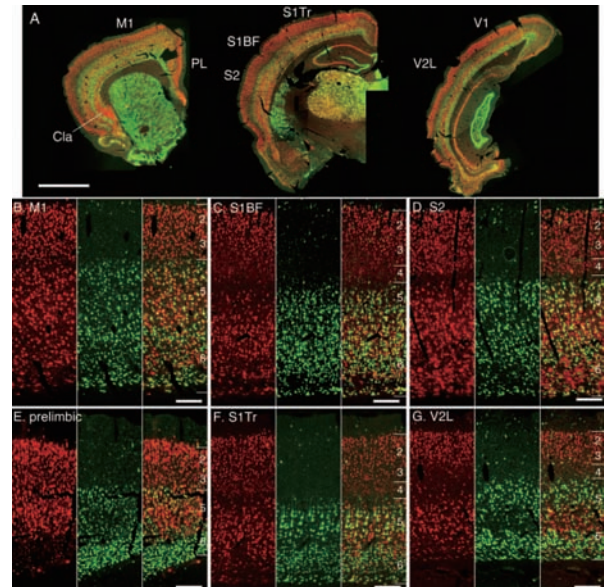


Figure 2. Expression patterns of *cck* and *pcp4* mRNAs in various cortical areas. A: Low magnified views of the double-ISH of *cck* (red) and *pcp4* (green) mRNAs in the rat brain. PL, prelimbic cortex; Cla, claustrum; M1, primary motor cortex; S1Tr, primary somatosensory cortex, trunk region; S1BF, primary somatosensory cortex, barrel field; S2, secondary somatosensory cortex; V1, primary visual cortex; V2L, secondary visual cortex lateral area. B–G: The magnified cortical areas labeled in panel A. Scale bars = 1 mm in A; 200 μm in B–G. (Watakabe et al., J Comp Neurol. 520, 3553-3573, 2012.)

relative abundance of *cck*(+) and *pcp4*(+) cells were quite distinctive across areas. For example, layer 6 of the prelimbic cortex was almost devoid of *cck*(+) neurons, and was occupied instead by corticothalamic *pcp4*(+) neurons. In the lateral areas, such as S2, there was an additional layer of *cck*(+) cells positioned below the *pcp4*(+) compartment. The claustrum, which has a tight relationship with the cortex, mostly consisted of *cck*(+)/*pcp4*(–) cells. The combination of gene markers and retrograde tracers revealed a distinct sublaminal organization, with conspicuous cross-area variation in the arrangement and relative density of corticothalamic connections. (Watakabe et al., J Comp Neurol. 520, 3553-3573, 2012.)

II. Visualization of cortical projection neurons with retrograde TET-off lentiviral vector.

We are interested in identifying and characterizing various projection neurons that constitute the neocortical circuit. For this purpose, we developed a novel lentiviral vector that carries the tetracycline transactivator (tTA) and the

transgene under the TET Responsive Element promoter (TRE) on a single backbone. By pseudotyping such a vector with modified rabies G-protein, we were able to express palmitoylated-GFP (palGFP) or turboFP635 (RFP) in the corticothalamic, corticocortical, and corticopontine neurons of mice. The high-level expression of the transgene achieved by the TET-Off system enabled us to observe characteristic elaboration of neuronal processes for each cell type (Figure 3). At higher magnification, we were able to observe fine structures such as boutons and spines as well. We also injected our retrograde TET-Off vector to the marmoset cortex, and therefore proved that this method can be used to label the long- long-distance cortical connectivity of the millimeter scale. In conclusion, our novel retrograde tracer provides an attractive option to investigate the morphologies of identified cortical projection neurons of various species (e.g., Figure 4) (Watakabe et al., PLoS One. 7, e46157, 2012).

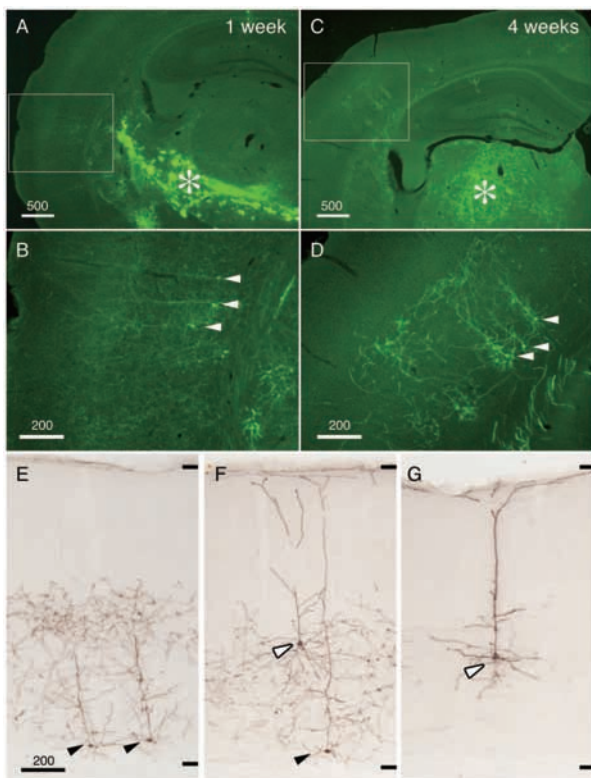


Figure 3. Retrograde infection of the corticothalamic cells by StTTrG/FuG-B vector. StTTrG/FuG-B vector was injected into the mouse thalamus. (A–D) After one week (for panels A and B) or four weeks (for panels C–G), the mouse was perfusion fixed and sliced at 40 μm thickness. The boxed areas in panels A and C were magnified in panels B and D, to show infection of corticothalamic neurons in layer 6 (indicated by arrowheads). The injection site is indicated by the asterisk (*). These images show the original green fluorescence of the infected cells. (E–G) The immunoperoxidase detection of the GFP-expressing cells. Bar: 500 μm (A and C), 200 μm (for others). Watakabe et al., PLoS One. 7, e46157. The caudal block of the marmoset brain was parasagittally sectioned to visualize the reciprocal connectivity between V1 and V2.

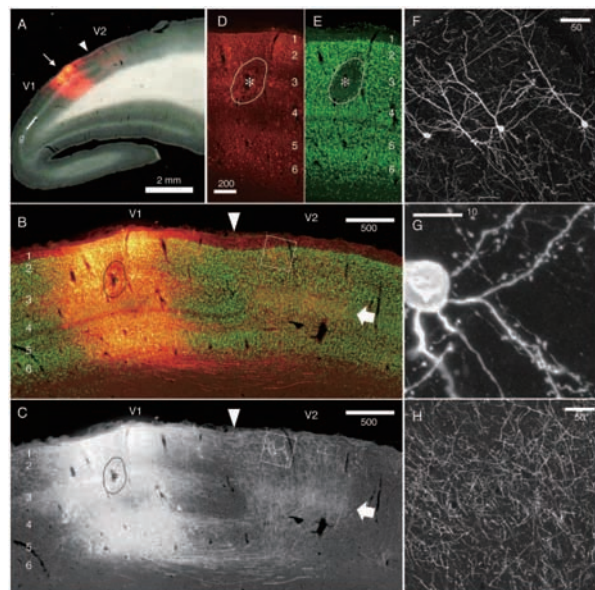


Figure 4. Reciprocal connectivity of marmoset V1 and V2 visualized by StTTrR/FuG-B vector.

(A) Dark field image overlaid with RFP fluorescence indicates the injection site. The V1/V2 border (shown by the arrowhead) was clearly delineated by the presence of the striate of Gennari (g). The arrow indicates the injection site. (B and C) The RFP signals around the injection site (red) are shown with NeuN counterstaining (green). The arrow indicates the plexus of V1 terminals in layer 4. The boxed region contains the retrogradely labeled V2 neurons with feedback projection to V1, which is magnified in panel F. The asterisk indicates the core of injection, where NeuN expression is lost by local damage. Only the RFP signals are shown in NeuN expression in panel C. (D and E) RFP signals (red) and NeuN stains (green) in the injection center. The contrast for the RFP signals is adjusted so that the cell bodies of the infected neurons can be delineated. Note that the lamina positions of the infected cells are restricted mostly to layers 2, 3 and 6. (F–H) Confocal images of RFP in V2. Panel F shows the cell bodies and dendrites of V2 neurons that project back to V1. (G) The spines of the basal dendrites originating from one of these cells. (H) The plexus of axon terminals concentrated in layer 4 of V2 (shown by the arrow). Bar: 2 mm for A; 500 μm for B and C; 200 μm for D and E; 10 μm for F and H; 50 μm for G.

Figures 3 and 4 from Watakabe et al., PLoS One. 7, e46157, 2012.

III. Behavioral analysis of *zfh2*-deficient mice.

Zfh2 (also known as *zfh-5*) encodes a transcription factor containing three homeobox domains and 18 Zn-finger motifs. We have reported that *Zfh2* mRNA is expressed mainly in differentiating neurons in the mouse brain and its expression level is negatively regulated by the antisense transcripts of *Zfh2* (Figure 5). Although the expression profile of *Zfh2* suggests that ZFH2 might have a role in a particular step of neuronal differentiation, the specific function of the gene has not been determined. We therefore generated a *Zfh2*-deficient mouse line and performed a comprehensive battery of behavioral tests to elucidate the function of ZFH2. Homozygous *Zfh2*-deficient mice showed several behavioral abnormalities, namely, hyperactivity, enhanced depression-like behaviors, and an aberrantly altered anxiety-like phenotype (e.g., Figure 6). These behavioral phenotypes suggest that ZFH2 might play roles in controlling emotional aspects through the function of monoaminergic neurons where ZFH2 is expressed.

Moreover, considering their phenotypes, the *Zfhx2*-deficient mice may provide a novel model of human psychiatric disorders. (Komine et al., PLoS One. 7, e53114, 2012)

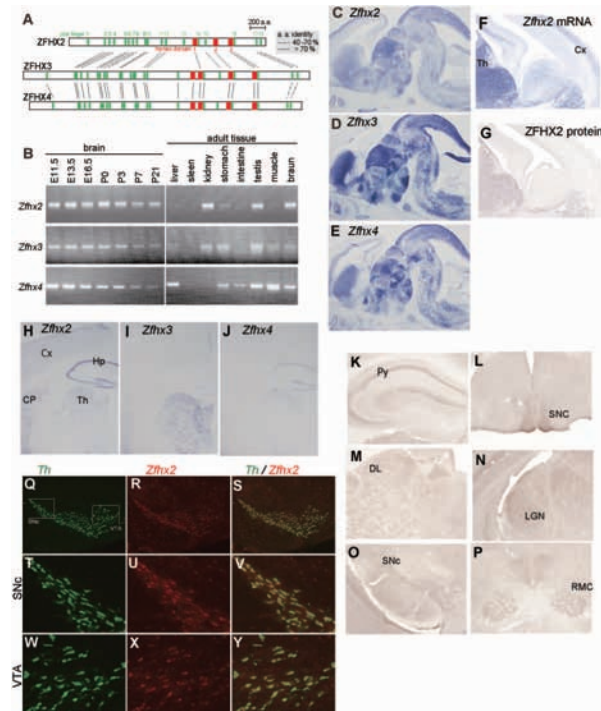


Figure 5. Structure and expression of mouse *Zfhx2*. (A) Structure of ZFHX2 and related proteins. ZFHX2 is a protein of 2562 amino acids containing 18 zinc fingers (green ovals) and three homeodomains (red squares). (B) *Zfhx2*, *Zfhx3*, and *Zfhx4* mRNA detected by semi-quantitative RT-PCR in various RNA sources. Note that cDNAs were amplified for 30 cycles for brains of different developmental stages, whereas cDNAs were amplified for 35 cycles for various adult tissues. (C–E) Expression of *Zfhx2* (C), *Zfhx3* (D), and *Zfhx4* (E) mRNA in the parasagittal sections of an E15.5 mouse brain. These three genes were expressed in substantially similar patterns with the highest expression level of *Zfhx3*. (F, G) Expression of *Zfhx2* mRNA (F) and the ZFHX2 protein (G) was compared on adjacent coronal sections of an E15.5 brain. mRNA expressed in the thalamic region (Th) was translated, whereas mRNA expressed in the cerebral cortex (Cx) was not translated: this situation made the expression patterns of ZFHX2 and ZFHX3 more alike in protein level than in mRNA level. (H–J) Expression of *Zfhx2* (H), *Zfhx3* (I), and *Zfhx4* (J) mRNA in the coronal sections of an adult brain. Cerebral cortex (Cx), hippocampus (Hp), thalamus (Th), caudate putamen (CP). Expression levels of all three genes were decreased compared with those in the embryonic brain, but *Zfhx2* maintained a higher level of expression than the others. (K–P) Expression of ZFHX2 protein in the adult brain. The pyramidal layer of the hippocampus (K, Py), the suprachiasmatic nucleus (L, SCN), laterodorsal thalamic nucleus (M, LD), lateral geniculate nucleus (N, LGN), substantia nigra pars compacta (O, SNC), and magnocellular part of the red nucleus suprachiasmatic (P, RMC). (Q–Y) Double-color in situ hybridization with *Zfhx2* (red) and tyrosine hydroxylase (Th) probes (green).

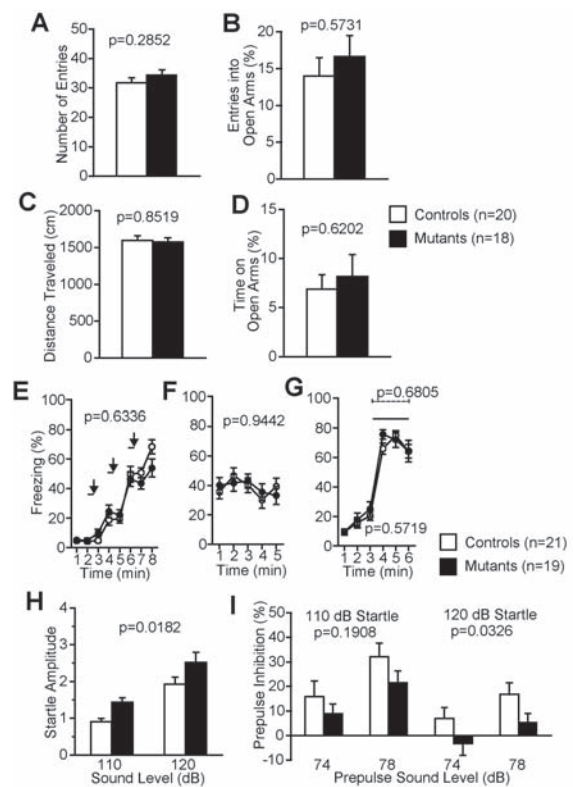


Figure 6. Locomotor activity measured in open field test. Distance traveled (A, B), stereotypic behavior (C), vertical activity (D), and time spent in the center area (E). Measurements are blocked in 5 min (A, C, D, and E) or in 1 min (B, shown only for the first 10 min). (Komine et al., PLoS One. 7, e53114, 2012)

Publication List

[Original papers]

- Kinoshita, M., Matsui, R., Kato, S., Hasegawa, T., Kasahara, H., Isa, K., Watakabe, A., Yamamori, T., Nishimura, Y., Alstermark, B., Watanabe, D., Kobayashi, K., and Isa, T. (2012). Genetic dissection of the circuit for hand dexterity in primates. *Nature* 487, 235-238.
- Komine, Y., Takao, K., Miyakawa, T., and Yamamori, T. (2012). Behavioral abnormalities observed in *zfhx2*-deficient mice. *PLoS ONE* 7, e53114.
- Takahata, T., Shukla, R., Yamamori, T., and Kaas, J.H. (2012). Differential expression patterns of striate cortex-enriched genes among Old World, New World, and prosimian primates. *Cereb. Cortex* 22, 2313-2321.
- Watakabe, A., Hirokawa, J., Ichinohe, N., Ohsawa, S., Kaneko, T., Rockland, K.S., and Yamamori, T. (2012). Area-specific substratification of deep layer neurons in the rat cortex. *J. Comp. Neurol.* 520, 3553-3573.
- Watakabe, A., Kato, S., Kobayashi, K., Takaji, M., Nakagami, Y., Sadakane, O., Ohtsuka, M., Hioki, H., Kaneko, T., Okuno, H., Kawashima, T., Bito, H., Kitamura, Y., and Yamamori, T. (2012). Visualization of cortical projection neurons with retrograde TET-off lentiviral vector. *PLoS ONE* 7, e46157.